

Deep learning of phase transitions with minimal examples

Ahmed Abuali,^{1,*} David A. Clarke,^{2,†} Morten Hjorth-Jensen,^{3,4}
Ioannis Konstantinidis,⁵ Claudia Ratti,¹ and Jianyi Yang⁵

¹*Physics Department, University of Houston, Houston, Texas 77204, USA*

²*Department of Physics and Astronomy, University of Utah, Salt Lake City, Utah 84112, USA*

³*Department of Physics and Astronomy and Facility for Rare Isotope Beams,
Michigan State University, East Lansing, Michigan 48824, USA*

⁴*Department of Physics and Center for Computing in Science Education, University of Oslo, N-0316 Oslo, Norway*

⁵*Computer Science Department, University of Houston, Houston, Texas 77204, USA*

(Dated: January 13, 2025)

Over the past several years, there have been many studies demonstrating the ability of neural networks and deep learning methods to identify phase transitions in many physical systems, notably in classical statistical physics systems. One often finds that the prediction of deep learning methods trained on many ensembles below and above the critical temperature T_c behave analogously to an order parameter, and this analogy has been successfully used to locate T_c and estimate universal critical exponents. In this work, we pay particular attention to the ability of a convolutional neural network to capture these critical parameters for the 2- d Ising model, when the network is trained on configurations at $T = 0$ and $T = \infty$ only. We apply histogram reweighting to the neural network prediction and compare its capabilities when trained more conventionally at multiple temperatures. We find that the network trained on two temperatures is still able to identify T_c and ν , while the extraction of γ becomes more challenging.

I. INTRODUCTION

A change of phase can often be characterized by an order parameter, an observable whose value is zero in one phase and nonzero in the other. When an order parameter can be identified, we call this phase change a phase transition. For phase transitions, there is a unique critical point or threshold in the control parameter at which the logarithm of the partition function $\log Z$ is not analytic. In other cases, there exist paths in the space of control parameters along which the phase changes while $\log Z$ experiences no non-analyticities. Such cases are called crossovers. Crossovers have no order parameter, and identifying a pseudocritical phase boundary, e.g. a pseudocritical temperature, is inherently ambiguous. Locating such boundaries is of special interest to the phase diagram of nuclear matter, whose change of phase from a gas of hadrons and their resonances to the quark-gluon plasma at zero net-baryon chemical potential is known to be a crossover [1].

Given the ambiguity of assigning a pseudocritical temperature, it may be illuminating to spot phase changes without having a physically motivated order parameter in mind. One approach is to use deep learning methods [2]. Deep learning and artificial neural networks have proven to be particularly well suited for phase classification tasks and locating critical points in classical spin systems, for both supervised and unsupervised learning, using a variety of architectures; see e.g. [3–13]. For studies of classical spin systems that use supervised learning,

one typically trains the deep learning model on multiple ensembles below and above the critical temperature T_c . These ensembles consist of configurations generated through Markov chain Monte Carlo (MCMC) simulations [14]. Configurations for ensembles with $T < T_c$ are labeled “ferromagnetic”, while ensembles with $T > T_c$ are labeled “paramagnetic”.

In the context of a crossover, this approach presents the inherent difficulty that there is no unique T_c , and therefore such a labeling is ambiguous in the region where the phase changes. To circumvent this issue, we explore using a convolutional neural network (CNN) [2] trained only at $T = 0$ and $T = \infty$, where the system is unambiguously ferromagnetic and paramagnetic, respectively. Moreover, rather than generating these two ensembles using MCMC simulations, we use the system’s known infinite-volume characteristics to create ensembles of exact magnetizations $|m| = 1$ and $m = 0$. We apply our approach to the 2- d Ising model and compare its capabilities to a more conventional supervised learning approach that trains on multiple ensembles around the transition region.

The outline of this paper is as follows. We start in Sec. II by describing our statistical physics model along with our general deep learning approach. In Sec. III, we describe our Monte Carlo data and deep learning model architecture and training method in detail. We show and discuss our findings in Sec. IV, wrapping up in Sec. V with a brief conclusion.

II. DEEP LEARNING AND THE ISING MODEL

We use deep learning methods like CNNs [2] to classify the phase of configurations belonging to the 2- d Ising model with zero external field, whose Hamiltonian is

* amabuali@uh.edu

† clarke.davida@gmail.com

given by

$$H = -J \sum_{\langle ij \rangle} \sigma_i \sigma_j, \quad (1)$$

where the brackets indicate a sum over nearest neighbors, $\sigma_i \in \{+1, -1\}$ is the spin at site i , and J is the nearest-neighbor interaction strength. We work in units with $J = k_B = 1$ and on square lattices of size $V = L^2$. The order parameter is the magnetization $m = V^{-1} \sum_i \sigma_i$. In the thermodynamic limit $L \rightarrow \infty$, the 2- d Ising model is analytically known to exhibit a second-order transition at a critical temperature [15]

$$T_c = \frac{2}{\log(1 + \sqrt{2})} \approx 2.269185, \quad (2)$$

at which the magnetic susceptibility

$$\chi = \beta V \left(\langle m^2 \rangle - \langle m \rangle^2 \right), \quad (3)$$

where $\beta = 1/T$, diverges. When $L < \infty$, χ peaks at a pseudocritical temperature $T_c(L)$. The approach of $T_c(L)$ to T_c as $L \rightarrow \infty$ is controlled by the universal critical exponent ν . In particular,

$$|T_c(L) - T_c| \sim L^{-1/\nu}. \quad (4)$$

Meanwhile, the peak height χ_{\max} scales according to the critical exponent γ as

$$\chi_{\max} \sim L^{\gamma/\nu}. \quad (5)$$

For the 2- d Ising universality class, these exponents are

$$\nu = 1, \quad \gamma = 1.75. \quad (6)$$

For discussions of these parameters, see for example Refs. [16–18].

The pioneering study in Ref. [3] trained a CNN to determine whether 2- d Ising-model configurations belong to the ferromagnetic or paramagnetic phase. After training on various lattice configurations, the authors of [3] tested their model with a different configuration; the prediction of the model P is a measure of how ferromagnetic the tested lattice configuration is, where $P \in [0, 1]$, with $P = 1$ being completely ferromagnetic and $P = 0$ being completely paramagnetic. They noticed that the average prediction $\langle P \rangle$, which can be interpreted as a probability that an ensemble belongs to the ordered phase, behaves analogously to m and hence used $\langle P \rangle$ to extract numerical values of T_c and ν to good accuracy. This analogy has been exploited in later studies, for example Ref. [19], with good results for various critical parameters. In such contexts, $\langle P \rangle$ is sometimes thought of as an “effective order parameter”. One can construct in analogy to Eq. (3) a prediction susceptibility

$$\chi_P \equiv \beta V \left(\langle P^2 \rangle - \langle P \rangle^2 \right). \quad (7)$$

In Ref. [19] it was noted that since P is a function of the configuration, it can be thought of as a thermodynamic observable and therefore can be reweighted [20, 21]. When reweighting, one infers the average value of an observable X at some β' from the known value at a sufficiently nearby point β through

$$\langle X \rangle_{\beta'} = \left\langle \frac{Z_\beta}{Z_{\beta'}} e^{(\beta - \beta')H} X \right\rangle_\beta, \quad (8)$$

where Z_β is the system’s partition function at β . We found reweighting to be useful in our context to accurately estimate the location of the peak in the prediction susceptibility and use it to help estimate statistical and systematic uncertainties.

III. SET UP AND DEEP LEARNING MODELS

We employ two training strategies in this work. The architecture we use is the CNN from Ref. [19]. The architecture is described in Appendix B of Ref. [19]. Our first strategy trains the CNN on 20 temperatures chosen above and below T_c , 10 in the range $2.44 \lesssim T \lesssim 3.13$ and 10 in the range $1.79 \lesssim T \lesssim 2.23$, corresponding to the β values listed in that work. We call this the “BAL20” model. Our second strategy trains the CNN on two ensembles only, corresponding to $T = 0$ and $T = \infty$. The $T = 0$ ensemble consists of 1000 configurations with $m = 1$ exactly and 1000 configurations with $m = -1$. Meanwhile, the $T = \infty$ ensemble consists of 2000 configurations where a randomly chosen set of half the spins is set to -1 while the other half is set to $+1$, yielding $m = 0$. We call this the “BAL” model. We emphasize that, in contrast to the BAL20 model, the BAL model is not trained on MCMC data. We implement our various CNN models using the machine-learning libraries Scikit-Learn [22] and Tensorflow [23] with Keras [24]. Our implementation of the CNNs can be accessed publicly on GitHub [25].

For efficient generation of 2- d Ising model configurations, we build on the code of Ref. [26]. We generate configurations of size $V = L^2$ for $L = 128, 200, 256, 360, 440, 512, \text{ and } 640$. The BAL model has an additional set of ensembles at $L = 760$, as it is significantly cheaper to train. For each L , we generate ensembles at many temperatures T . For each T we generate $N_{\text{conf}} = 2000$ configurations that are extremely well separated in Markov time; in particular, each measurement is separated by $5L^2$ sweeps. Ensemble averages $\langle X \rangle$ are estimated by

$$\langle X \rangle = \frac{1}{N_{\text{conf}}} \sum_{i=1}^{N_{\text{conf}}} X_i. \quad (9)$$

Jackknife resampling, reweighting, fitting for the exponent γ , and the subsequent model averaging discussed in Sec. IV are carried out using software of the Analysis-Toolbox [27].

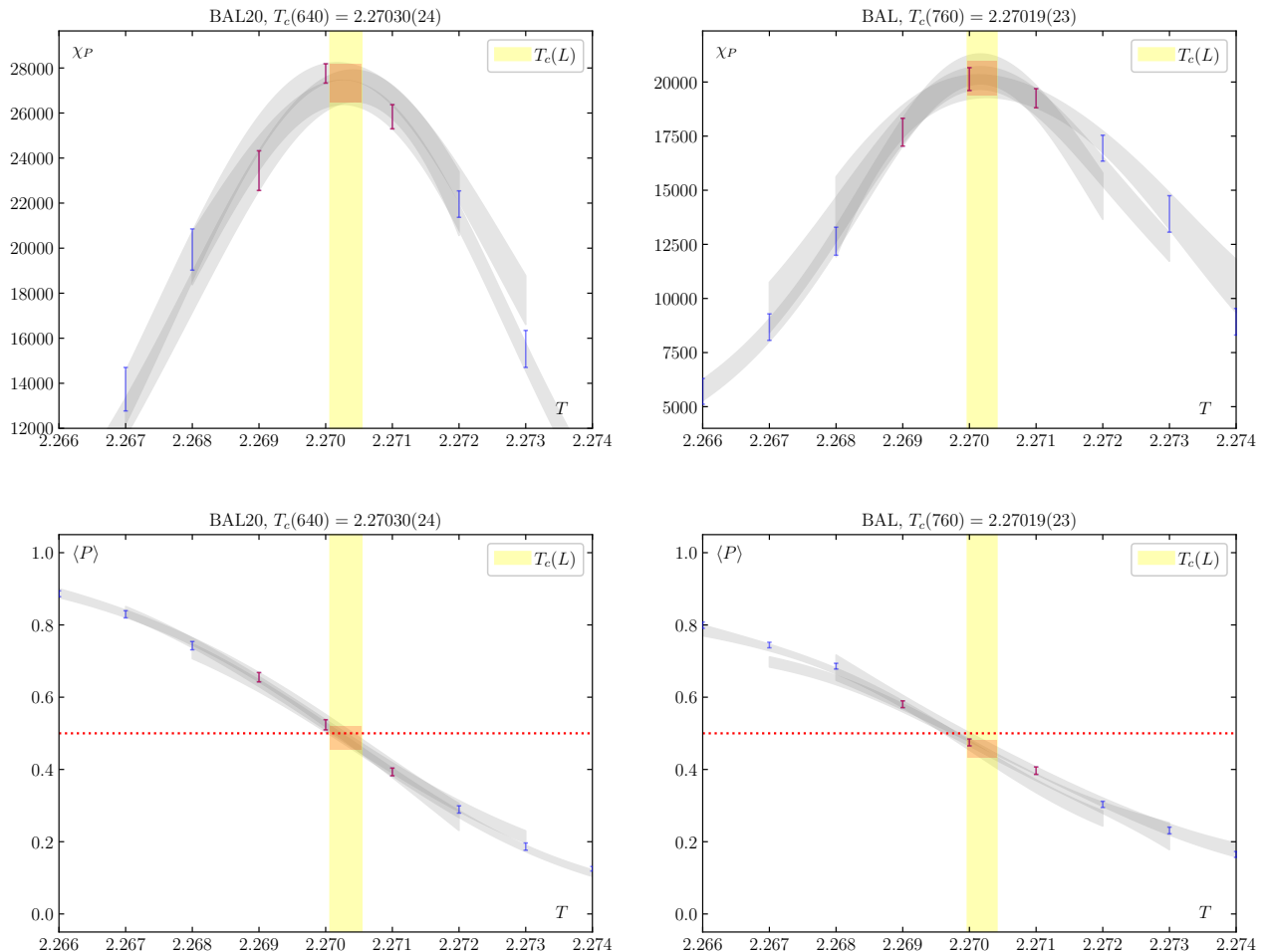


FIG. 1. Reweighting of χ_P (top) and P (bottom) for the BAL20 (left) and BAL (right) models using the largest lattice available to each model. Blue data indicate the output of the CNN. Red data indicate starting points for the reweighting curves, which are shown in gray. The yellow band indicates the estimated $T_c(L)$. In orange, we show the reweighted observable evaluated at $T_c(L)$ along with its associated total uncertainty. The red, dotted line indicates $P = 0.5$.

IV. RESULTS AND DEEP LEARNING MODEL PERFORMANCE

Under the assumption that $\langle P \rangle$ behaves as an effective order parameter, we estimate pseudo-critical temperatures $T_c(L)$ using the peak location of the predicted susceptibility χ_P for each L . We reweigh χ_P according to Eq. (8) to find the peak. To estimate statistical uncertainties, we resample our data using 40 jackknife bins. The peak location found by reweighting depends on the starting point β used in Eq. (8). We reweigh using points closest to the maximum, then estimate a systematic uncertainty equal to the spread of the $T_c(L)$ found for each β . The total error is computed by adding the statistical and systematic uncertainties in quadrature.

This process is illustrated for each CNN model using the largest lattices in Fig. 1 (top). The range in β for which reweighting is reliable decreases exponentially with

V ; that the reweighting curves agree on our largest volumes shows that our reweighting procedure is well controlled. In Fig. 1 (bottom) we show the corresponding reweighted predictions. We find $T_c(L)$ to be at or close to the region where $\langle P \rangle = 0.5$.

Armed with estimates for $T_c(L)$ and χ_{\max} , we can extract critical exponents. In Fig. 2 we show results for the BAL20 and BAL models. We begin by extracting T_c and ν by carrying out a fit using Eq. (4). To achieve numerical stability, we recast this equation as

$$\log L = -\nu \log |T_c(L) - T_c|. \quad (10)$$

Since our uncertainties are in the independent variable T , we carry out this fit using orthogonal distance regression¹. Results of the fits are in Fig. 2 (left). As was

¹ We do our orthogonal distance regression using the software of

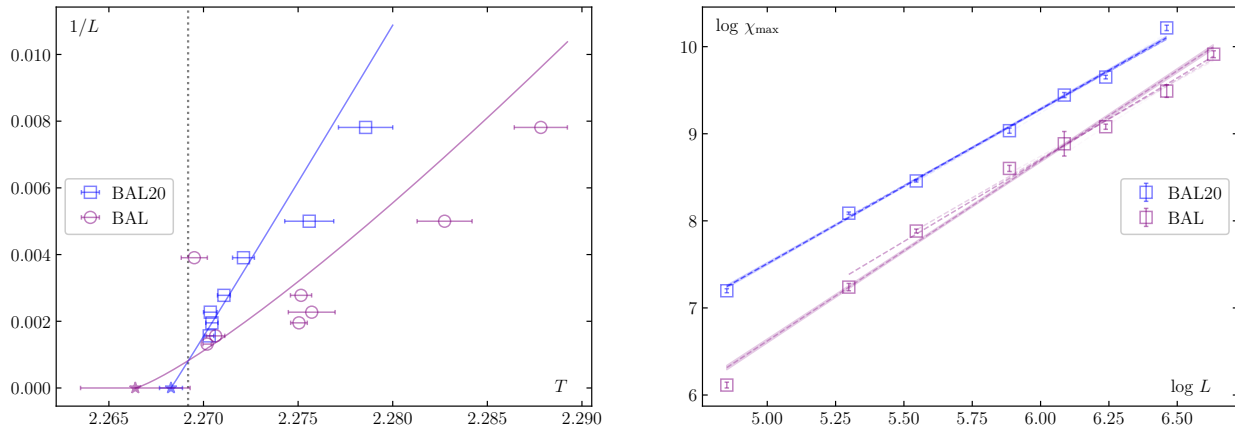


FIG. 2. Extraction of T_c and critical exponents for the 2- d Ising model using the CNN output layer. *Left*: Extraction of T_c and ν . The grey, dotted line indicates the theoretical value Eq. (2). *Right*: Extraction of γ . Bands show a linear fit to all data with error. Dashed lines indicate linear fits neglecting the smallest lattices, which enter the BMA. The transparency of each line indicates $\text{pr}(M_n|D)$ with darker lines indicating greater model weight.

reported in Ref. [19], the results for the BAL20 model are quite good. We find

$$T_c^{\text{BAL20}} = 2.26828(61), \quad \nu^{\text{BAL20}} = 1.017(41), \quad (11)$$

with a residual variance of 1.547, which is in excellent agreement with Eqs. (2) and (6). We found the finite-size scaling of the BAL model not to be described as well by the fit of Eq. (10); in particular the fit has a residual variance of 28.982. This is due to the outlier at $L = 256$ along with the fact that the BAL model seems to find the same $T_c(L)$ within error for $L = 360, 440, \text{ and } 512$. Still, our fit yields

$$T_c^{\text{BAL}} = 2.2664(29), \quad \nu^{\text{BAL}} = 1.21(12), \quad (12)$$

which are both statistically compatible with the analytic results.

Next we show the extraction of γ using Eq. (5), shown in Fig. 2 (right). This exponent is extracted using conventional least-squares methods. The BAL20 fit gives

$$\left(\frac{\gamma}{\nu}\right)^{\text{BAL20}} = 1.776(17) \quad (13)$$

with a $\chi^2/\text{d.o.f.} = 8.60$, in agreement with the known result. By contrast the BAL model seems unable to capture γ . We find

$$\left(\frac{\gamma}{\nu}\right)^{\text{BAL}} = 2.069(24) \quad (14)$$

with a $\chi^2/\text{d.o.f.} = 18.25$. While this number is not statistically compatible with the known result, χ_{\max} for this

CNN model behaves qualitatively reasonably. We see $\log \chi_{\max}$ scales very roughly linearly with $\log L$ with a slope roughly 16% larger than the analytic value.

The finite-size behavior of Eqs. (4) and (5) holds for large L . The predictions from the different CNN models P^{BAL20} and P^{BAL} represent different observables, and hence there is no guarantee that the onset of finite-size scaling will occur starting with the same minimum L for both quantities. To understand the extent to which the inability to capture γ/ν can be explained by a small finite-size scaling window, we try fits that leave out progressively larger L values among the smallest lattices.

Each combination of analysis choices, in this case the fit of Eq. (5) equipped with choosing a number of L data to prune, defines a statistical model² M_n . To compute an average from this process we employ Bayesian model averaging (BMA) [30–32],

$$\langle \gamma/\nu \rangle_{\text{BMA}} = \sum_{n=1}^{N_M} \langle \gamma/\nu \rangle_n \text{pr}(M_n | D), \quad (15)$$

where the sum runs over models M_n , N_M is the number of models, and $\langle \gamma/\nu \rangle_n$ is the result for γ/ν found in model M_n . The model weight, that is the probability of the model M_n given the data D , is

$$\text{pr}(M_n | D) = \text{pr}(M_n) \exp \left[-\frac{1}{2} (\chi_n^2 + 2k + N_{\text{cut}}) \right], \quad (16)$$

² We have tried to distinguish the use of the word “model” in this sense from deep-learning models by calling the latter “deep learning model”, “BAL model”, or “BAL20 model”.

SciPy [28]. These fits are cross-checked using GVAR [29].

where $\text{pr}(M_n)$ is the prior probability of model M_n , χ_n^2 gives³ χ^2 evaluated for model M_n , k is the number of fit parameters, and N_{cut} is the number of sizes L trimmed from the data set. The model weight penalizes poor fits, large numbers of fit parameters, and cutting away data. For our case, $k = 2$, and we take $\text{pr}(M_n) = 1/N_M$, a choice which gives no *a priori* preference for one model over another. The variance in the BMA average $\langle\gamma/\nu\rangle$ is computed through

$$\sigma_{\text{BMA}}^2 = \sum_{n=1}^{N_M} \sigma_n^2 \text{pr}(M_n | D) + \sum_{n=1}^{N_M} \langle\gamma/\nu\rangle_n^2 \text{pr}(M_n | D) - \langle\gamma/\nu\rangle_{\text{BMA}}^2, \quad (17)$$

where σ_n^2 is the variance in $\langle\gamma/\nu\rangle_n$. This can be interpreted as a statistical uncertainty combined with a systematic measure of the model spread, given by the second and third terms.

The fits for each M_n entering the BMA are indicated by dashed lines in Fig. 2 (right), where the transparency of the dashed line indicates $\text{pr}(M_n | D)$. Generally, increasing the minimum L used decreases the slope and model weight. The BMA yields

$$\left(\frac{\gamma}{\nu}\right)_{\text{BMA}}^{\text{BAL}} = 1.92(13). \quad (18)$$

The central value decreases compared to Eq. ((14)). It remains high compared to the analytic result, but is now compatible within the substantially larger uncertainty. This may suggest that $\chi_{\text{max}}^{\text{BAL}}$ only enters its finite-size scaling range for much larger lattices. For comparison, we also carry out a BMA for the BAL20 model. Again the fits are indicated in the figure using dashed lines. In contrast to the BAL model, the fits are much more closely aligned; the fits with non-negligible model weight overlap with the original fit, and we find

$$\left(\frac{\gamma}{\nu}\right)_{\text{BMA}}^{\text{BAL20}} = 1.786(65). \quad (19)$$

When exploring the finite-size scaling of a system using m -derived quantities, one can extract a critical exponent β , related to m via

$$\langle m \rangle |_{T_c(L)} \sim L^{-\beta/\nu}. \quad (20)$$

Such a relation cannot be expected from the average prediction $\langle P \rangle$ if it is to be interpreted as a probability of being ferromagnetic. In particular since the pseudocritical temperature $T_c(L)$ is the point at the phase boundary,

configurations at this temperature ought to be equally often classified as ferromagnetic and paramagnetic, and hence one expects

$$\langle P \rangle |_{T_c(L)} = \frac{1}{2}. \quad (21)$$

As mentioned earlier, we see in Fig. 1 (bottom) that $\langle P \rangle$ at $T_c(L)$ is compatible with 0.5 within error for both deep learning (CNNs here) models.

Our empirical study is unable to discern the exact mechanism that lowers the ν - T_c fit quality for the BAL model and increases the difficulty of finding γ . Clearly, this deep learning model is given significantly less information during training compared to BAL20; in particular it lacks any example at intermediate temperatures. We are therefore impressed by the ability of the BAL model to locate T_c , find ν , and to some degree find γ using only the knowledge of what $T = 0$ and $T = \infty$ configurations must look like, combined with the fact that the phase transition is of second order.

V. SUMMARY AND OUTLOOK

In this paper, we studied the capabilities of a CNN (BAL model) using a minimal set of examples, specifically examples at $T = 0$ and $T = \infty$, comparing its performance to the same CNN trained on 20 temperatures near T_c (BAL20 model). We confirm the findings of Ref. [19] that the output layer can be reweighted and that the BAL20 model easily extracts T_c , ν , and γ . The BAL model finds T_c and ν , albeit with poor fit quality and correspondingly higher uncertainty. A BMA of fits for γ for the BAL model prefers fits over our largest volumes. This behavior may be due in part to finite-size scaling setting in at larger L than for the BAL20 model and in part to the performance of the BAL model itself. The larger uncertainties, lower fit qualities, and relative difficulty extracting γ exposes to some extent the role of examples at intermediate temperatures.

In this study, we looked at only one architecture to focus on the effect the choice of examples has on a successful extraction of critical parameters. It could be that a different architecture would be better optimized for having two examples only. Further architectures will be explored in future work.

We find our results encouraging for eventual application of supervised learning to systems with crossovers. In particular, the ability of a minimally trained model to find not just T_c but to some degree ν and γ indicates that the model still learns salient features of configurations that flag a change of phase. Thinking about the QCD transition, one may imagine training at very high temperatures and very low temperatures, using the outputs of deep learning methods like CNNs to define a new observable that could be used to define a pseudocritical temperature.

³ More precisely this is χ_{data}^2 , the χ^2 computed not taking into account any priors on fit parameters. We use no priors for fit parameters in this study, so we do not make the distinction.

ACKNOWLEDGMENTS

We acknowledge fruitful discussions with Gregory Morrison, Kevin Bassler, and Ricardo Vilalta. The research reported in this work made use of computing facilities of the USQCD Collaboration, which are funded by the Office of Science of the U.S. Department of Energy. DAC was supported in part by the U.S. Department of Energy, Office of Science, under the Funding Opportunity Announcement Scientific Discovery through Advanced Computing: High Energy Physics, LAB 22-2580 and by the National Science Foundation under Grant No. PHY23-10571. The authors acknowledge the use of the Carya Cluster and the advanced support from the Re-

search Computing Data Core at the University of Houston to carry out the research presented here. This material is based upon work supported by the National Science Foundation under grants No. PHY-2208724 and PHY-2116686, and within the framework of the MUSES collaboration, under Grant No. OAC-2103680. This material is also based upon work supported by the U.S. Department of Energy, Office of Science, Office of Nuclear Physics, under Award Number DE-SC0022023, as well as by the National Aeronautics and Space Agency (NASA) under Award Number 80NSSC24K0767. MHJ was supported in part by the U.S. Department of Energy under award number DE-SC0024586.

-
- [1] Y. Aoki, G. Endrodi, Z. Fodor, S. D. Katz, and K. K. Szabo, The Order of the quantum chromodynamics transition predicted by the standard model of particle physics, *Nature* **443**, 675 (2006), [arXiv:hep-lat/0611014](#).
- [2] I. Goodfellow, Y. Bengio, and A. Courville, *Deep Learning* (The MIT Press, Cambridge, Massachusetts, 2016).
- [3] J. Carrasquilla and R. G. Melko, Machine learning phases of matter, *Nature Phys.* **13**, 431 (2017), [arXiv:1605.01735 \[cond-mat.str-el\]](#).
- [4] L. Wang, Discovering phase transitions with unsupervised learning, *Phys. Rev. B* **94**, 195105 (2016).
- [5] E. P. L. van Nieuwenburg, Y.-H. Liu, and S. D. Huber, Learning phase transitions by confusion, *Nature Phys.* **13**, 435 (2017), [arXiv:1610.02048 \[cond-mat.dis-nn\]](#).
- [6] W. Hu, R. R. P. Singh, and R. T. Scalettar, Discovering phases, phase transitions, and crossovers through unsupervised machine learning: A critical examination, *Phys. Rev. E* **95**, 062122 (2017).
- [7] S. J. Wetzel, Unsupervised learning of phase transitions: From principal component analysis to variational autoencoders, *Phys. Rev. E* **96**, 022140 (2017).
- [8] S. Foreman, J. Giedt, Y. Meurice, and J. Unmuth-Yockey, Examples of renormalization group transformations for image sets, *Phys. Rev. E* **98**, 052129 (2018), [arXiv:1807.10250 \[hep-lat\]](#).
- [9] G. Cossu, L. Del Debbio, T. Giani, A. Khamseh, and M. Wilson, Machine learning determination of dynamical parameters: The Ising model case, *Phys. Rev. B* **100**, 064304 (2019), [arXiv:1810.11503 \[physics.comp-ph\]](#).
- [10] S. Shiba Funai and D. Giataganas, Thermodynamics and Feature Extraction by Machine Learning, *Phys. Rev. Res.* **2**, 033415 (2020), [arXiv:1810.08179 \[cond-mat.stat-mech\]](#).
- [11] N. Walker, K.-M. Tam, and M. Jarrell, Deep learning on the 2-dimensional Ising model to extract the crossover region with a variational autoencoder, *Sci. Rep.* **10**, 13047 (2020).
- [12] X.-Q. Han, S.-S. Xu, Z. Feng, R.-Q. He, and Z.-Y. Lu, Framework for Contrastive Learning Phases of Matter Based on Visual Representations, *Chin. Phys. Lett.* **40**, 027501 (2023), [arXiv:2205.05607 \[cond-mat.dis-nn\]](#).
- [13] S. Bae, E. Marinari, and F. Ricci-Tersenghi, A very effective and simple diffusion reconstruction for the diluted Ising model, (2024), [arXiv:2407.07266 \[cond-mat\]](#).
- [14] W. R. Gilks, R. S., and D. E. Spiegelhalter, *Markov Chain Monte Carlo in Practice* (Chapman and Hall/CRC, 1995).
- [15] L. Onsager, Crystal statistics. 1. A Two-dimensional model with an order disorder transition, *Phys. Rev.* **65**, 117 (1944).
- [16] J. Cardy, *Scaling and Renormalization in Statistical Physics* (Cambridge University Press, 1996).
- [17] H. Stanley, *Introduction to Phase Transitions and Critical Phenomena* (Oxford University Press, 1971).
- [18] M. Newman and G. Barkema, *Monte Carlo Methods in Statistical Physics* (Clarendon Press, 1999).
- [19] D. Bachtis, G. Aarts, and B. Lucini, Extending machine learning classification capabilities with histogram reweighting, *Phys. Rev. E* **102**, 033303 (2020), [arXiv:2004.14341 \[cond-mat.stat-mech\]](#).
- [20] A. M. Ferrenberg and R. H. Swendsen, New Monte Carlo Technique for Studying Phase Transitions, *Phys. Rev. Lett.* **61**, 2635 (1988).
- [21] A. M. Ferrenberg and R. H. Swendsen, Optimized Monte Carlo analysis, *Phys. Rev. Lett.* **63**, 1195 (1989).
- [22] F. Pedregosa *et al.*, Scikit-learn: Machine learning in Python, *Journal of Machine Learning Research* **12**, 2825 (2011).
- [23] M. Abadi *et al.*, *TensorFlow: Large-scale machine learning on heterogeneous systems* (2015), software available from tensorflow.org.
- [24] F. Chollet *et al.*, Keras, <https://keras.io> (2015).
- [25] A. Abuali, CNN-Ising2D-BAL public code repository, https://github.com/clarkedavida/CNN_Ising2D_BAL.
- [26] J. Romero, M. Bisson, M. Fatica, and M. Bernaschi, A Performance Study of the 2D Ising Model on GPUs, (2019), [arXiv:1906.06297 \[cs\]](#).
- [27] D. A. Clarke, L. Altenkort, J. Goswami, and H. Sandmeyer, Streamlined data analysis in Python, *PoS LATTICE2023*, 136 (2024), [arXiv:2308.06652 \[hep-lat\]](#).
- [28] P. Virtanen *et al.*, SciPy 1.0—Fundamental Algorithms for Scientific Computing in Python, *Nature Meth.* **17**, 261 (2020), [arXiv:1907.10121 \[cs.MS\]](#).
- [29] G. Lepage, C. Gohlke, and D. Hackett, [gplepage/gvar v11.10](#) (2022).
- [30] W. I. Jay and E. T. Neil, Bayesian model averaging for analysis of lattice field theory results, *Phys. Rev. D* **103**, 114502 (2021), [arXiv:2008.01069 \[stat.ME\]](#).

- [31] E. T. Neil and J. W. Sitison, Improved information criteria for Bayesian model averaging in lattice field theory, *Phys. Rev. D* **109**, 014510 (2024), [arXiv:2208.14983 \[stat.ME\]](#).
- [32] E. T. Neil and J. W. Sitison, Model averaging approaches to data subset selection, *Phys. Rev. E* **108**, 045308 (2023), [arXiv:2305.19417 \[stat.ME\]](#).